



Seismic Noise Analysis of Four Broadband Seismic Stations in Central Part of Iraq Using Probabilistic Power Spectral Density (PPSD)

Taif Qusay^{1*}, Najah Abd²

¹ University of Baghdad College of Science / Department of Geology, Iraq, Baghdad

² University of Baghdad College of Science / Lab of Seismology and Spatial Data Analysis, Iraq, Baghdad

Received: 20/10/2024

Accepted: 19/2/2025

Published: xx

Abstract

Seismic noise analysis is crucial to enhance the reliability of earthquake monitoring networks. Therefore, in this paper, we investigated the ambient seismic noise at four seismic stations in central Iraq, namely Karbala (KAR2), Kut (KUT1), Diyala (DYL1), and Baghdad (BGD1) over a period of one year, by analysing the seismic noise using power spectral density (PSD) and probability density function (PDF) techniques and then comparing the analysis results with Peterson's models. Our results indicate that most of the stations are within the acceptable noise levels according to Peterson's model. However, the Karbala (KAR2) station consistently exceeds the New High Noise Model (NHNM) standards over the long periods range. A new station was installed in Karbala, and its noise analysis was calculated, but the results were similar to those of the old station. Therefore, the station location is not ideal for earthquake monitoring and should be moved to a different location.

Keywords: Seismic-noise Analysis, Ambient seismic noise, Seismic Stations, Power Spectral Density (PSD), Probability Density Function (PDF).

تحليل الضوضاء الزلزالية لأربع محطات زلزالية ذات نطاق عريض في الجزء الأوسط من العراق باستخدام كثافة الطيف الاحتمالي للقدرة (PPSD)

طيف قصي^{1*}, نجاح عبد²

¹ قسم الجيولوجيا، كلية العلوم، جامعة بغداد، العراق، بغداد

² مختبر الزلزال وتحليل البيانات المكانية، كلية العلوم، جامعة بغداد، العراق، بغداد

الخلاصة

إن تحليل الضوضاء الزلزالية أمر بالغ الأهمية لتعزيز موثوقية شبكات رصد الزلزال. لذلك، قمنا في هذا البحث بالتحقيق في الضوضاء الزلزالية المحيطة في أربع محطات زلزالية في وسط العراق، وهي كربلاء (KAR2)، والكوت (KUT1)، وديالى (DYL1) وبغداد (BGD1) على مدى عام واحد، والتي تضمنت تحليل الضوضاء الزلزالية باستخدام تقنيات كثافة الطيف للقدرة (PSD) ودالة كثافة الاحتمال (PDF) ثم مقارنة نتائج التحليل بنماذج بيترسون. تشير نتائجنا إلى أن معظم المحطات تقع ضمن مستويات الضوضاء المقبولة وفقاً لنموذج بيترسون. ومع ذلك، فإن محطة كربلاء (KAR2) تتجاوز باستمرار معايير نموذج الضوضاء العالمية

* Email: Taif.Qassi1608a@sc.uobaghdad.edu.iq

الجديد (NHNM) على مدى فترات طويلة. تم تركيب محطة جديدة في كربلاء وتم حساب تحليل الضوضاء للمحطة ولكن النتائج كانت مماثلة أيضاً للمحطة القديمة. لذلك، فإن المحطة ليست متألية لمراقبة الزلزال ويجب نقلها إلى موقع مختلف.

1. Introduction

The most important criterion for any seismic network is establishing its capacity to detect seismic events. This detection capability represents the performance characteristics of the network's stations, with the station detection threshold serving as a quantitative measure of earthquake detection capability [1] [2]. Modern equipment is incredibly sophisticated and capable of detecting even tiny occurrences. Although seismic recordings inherently include noise, it is essential to identify the sources of this noise to reduce its influence effectively. The detected noise on the seismic trace is most likely caused by seismic equipment, natural vibrations of the earth (ambient seismic noises), or any cultural (artificial) source near the station. Tides can cause ambient noise, ocean waves hitting the coast, turbulent wind, wind impacts on trees and buildings, and traffic or made by human noises [3]. Over several years, investigations have revealed that noise exhibits temporal and spatial variability with a significant frequency dependence. It is regarded as a function that depends on location and time, changing according to the day and season. Typically, the ambient noise should be lower than the seismic noise. However, identifying this can be difficult unless one has an understanding of the unique noise characteristics at a particular station [2].

Seismic noise analysis is crucial in the middle of Iraq because of the continuous environmental fluctuations and human activities that generate noise, which impacts seismic stations' accuracy in monitoring earthquakes. Central Iraq's geography is diverse, with different terrains, climates, and increased human interaction. The region is influenced by severe environmental perturbations, including wind, sandstorms, and temperature fluctuations that affect the level of ambient seismic noise. Also, cultural factors such as industrialization, construction, and transport infrastructure create significant cultural noise that may interfere with or weaken seismic signals [4, 5]. Therefore, based on the analysis of the stations, it is possible to identify the specific zones with a high level of noise, which will allow for the appropriate approach to targeting site characteristics. It can also assist in determining the most suitable locations and vault designs for installing seismic stations to increase monitoring efficiency. This significantly enhances the reliability of the gathered data and the seismic risks for the future, thereby increasing the level of preparation and response to earthquakes in central Iraq [6].

Power Spectral Density (PSD) computation is one of the most traditional approaches to seismic-noise analysis since it reveals the power distribution across the various frequencies. This technique assesses background noise in the seismic recording environment and is used as a benchmark across time. This steady reference is important when checking how long a seismometer takes before it is ready to provide usable data [7]. Thus, evaluating the noise spectrum allows for determining the expected operational performance of a seismic station. When there are variations in the analysis results, such as instrument malfunction or inconsistencies in the response data, the noise spectrum calculation and comparison with the standard spectrum can quickly reveal any significant changes in the system [8].

The aim of this paper includes the following: (1) Analyse the features and origin of seismic noise recorded at four broadband stations based in the middle of Iraq. (2) Assess the efficiency of these stations to confirm the credibility of the data captured and improve the ability of these stations to identify earthquake signals. (3) Investigate the characteristics of seismic noise at particular sites by calculating the PSD of the background noise at each station and comparing these with Peterson's (1993) global model of seismic noise.

2. Literature Review

Recent seismic research has increasingly centred on evaluating seismic noise and station performance, particularly emphasizing the PSD method. This method has been employed across various studies to analyse the ambient noise levels of each station. Grecu et al. [9] investigated the site noise characteristics and variations at different seismic stations in the Romanian-Bulgarian cross-border region over three years. The Power Spectral Density (PSD) and Probability Density Function (PDF) methods were used to examine the fluctuations in noise levels between daytime and nighttime and during the seasons at different seismic stations. Compared to the Peterson model, significant variations in noise levels were observed throughout the day, especially during working days, indicating anthropogenic sources. Seasonal variations were also observed, with increased noise levels during the winter season and significant differences in the double-frequency peak (DFP) related to the weather conditions in the Black Sea. Hafiez et al. [2] examined nine broadband stations in northern Egypt for seismic noise analysis, focusing on ambient noise levels and site characteristics. The study utilized the PSD estimator and PDF within the PQLX (a tool for visualizing time-series data in of the three formats: miniseed- segy- sac) software to evaluate background noise in the vertical component over periods ranging from 0.2 to 180 seconds for one year. Comparing their assessment with Peterson's models, the researchers established variations in noise level among the stations, some displayed low detectability and high noise, especially at higher frequencies, due to human activities around the stations. Further, the H/V (horizontal/vertical) component of the noise signal method was applied to compare the site amplification, and it was noted that some stations might have to be shifted due to high noise levels. Rahayu et al. [10] used the PSD and PDF methods to analyse the efficiency of three mini-seismic stations located in Northern Sumatra during the Padang Lawas earthquake. Seismic waveform data in the vertical and horizontal components were recorded in the Mini Standard for the Exchange of Earthquake Data (miniSEED) format and then transformed into the Seismic Analysis Code (SAC) format. The PSD and PDF methods were then employed to analyse the amplitude and probability density of the collected data. Comparing the amplitudes of signals to Peterson's models, the signal amplitudes ranged between -190dB to -110dB, and the probability densities ranged between 15%-30%, implying that the performance of the stations was close to the NLNM model; this is an indication of the stations' efficiency in detecting seismicity. Sinambela et al. [11] assessed the effectiveness of four broadband GFZ seismic stations in Sumatra with data collected during the Tarutung earthquake in 2019. The PSD and PDF techniques were employed to assess the ambient seismic noise of each station, which was calculated through the ObsPy Python library. Compared with Peterson's models, the authors have established that one station had the lowest background noise levels, which was close to the NLNM in the 2-10 s frequency range. The remaining stations recorded higher noise levels similar to the NHNM, with the PSD and PDF estimations showing significant background noise in the 1-20 s frequency range associated with cultural noise. Saha and Srinagesh [12] employed the PSD method to assess seismic noise characteristics at a broadband seismic site in East Antarctica during summer and winter. The data was recorded in Mini Standard for the Exchange of Earthquake Data (miniSEED) format and filtered from earthquake signals and instrument calibration pulses. The data was then translated to PSD equivalents in the frequency domain using the SQLX tool, and PDFs were created to analyse the performance of the station. Compared to Peterson's models, the results presented lower noise levels in winter than in summer, demonstrating the role of seismic vault design and seasonal analysis for low-noise seismic data acquisition. Hakim et al. [13] evaluated the seismic data quality at 15 stations during the Flores earthquake using the Probability Power Spectral Density (PPSD) class to compute PSD and PDF. In the data processing, mean trend removal was done, tapers were used, and FFT was applied to properly compute the PSD and construction PDF for respective

stations using the Obspy Python library. A comparison with Peterson's models revealed that most stations had noise levels within the acceptable NHNM to NLNM range, indicating good data quality. However, PPSD results from one station fell below the NLNM model due to metadata errors, leading to a recommendation to exclude this station from future earthquake analyses. Agusdiansyah et al. [14] employed the PSD method to study the noise characteristics of micro-earthquake stations on Bangka Island and to compare analyses of data collected from September 2021 with the data from 2014 to evaluate the performance of each station. The analysis showed that all the stations had good performance with noise levels consistent with NHNM and NLNM ranges at periods ranging from 0.1-1 sec, except one station showed a low likelihood of noise occurrence with significant power exceeding the NHNM level. Meanwhile, the noise levels at periods ranging from 1-10 sec were reduced due to micro-seismic activity. Jha [15] assessed seven broadband stations in the Western Ghats of India for seismic noise analysis using PSD and PDF calculated through PQLX software. According to their study, three stations were found to have high cultural interference, especially in the daytime, because of vehicle movement. Seasonal changes were also recorded at other stations, with high noise levels during the monsoon period, particularly in coastal areas. However, the level of noise observed at all the stations was within the Peterson standards models, which indicates the reliability of the data from these broadband seismological stations.

3. Seismic Noise Analysis

Seismic data quality is of paramount importance when it comes to analysing earthquakes, and one of the aspects that influence data quality is the noise level at each station. Several factors give rise to this noise, such as earthquake surface waves, cultural noise as well as oceanic storms. As proposed by Aster et al. [16] and McNamara and Buland [17], Analysing noise levels at seismic stations is an effective method for assessing their functionality. This approach should be utilized as a preliminary measure to reduce seismic noise signals. The computation of the PSD and PDF of a seismic signal, when compared to the New High Noise Model (NHNM) and New Low Noise Model (NLNM) curves introduced by Peterson [18], provides valuable information. These curves show the extreme range of cumulative ground acceleration estimated from noise and quiet segments of 75 global digital stations [19]. The Peterson curves have remained the most used for assessing noise levels at seismic stations. To compare spectra correctly, it is advisable to adhere to the definition provided by Peterson [18]. This method is significant in revealing the noise level and checking the system response accuracy, a key factor for identifying seismic stations. At present, determining the level of ambient seismic noise is an everyday process of assessing potential sites for deploying a station. Noise measurement is usually done at every site before installation of the station. It should be done on a regular basis after installation to assess any changes that may have occurred in noise levels or any other technical problems [20].

In order to reduce noise levels in a seismometer, it is important to choose the right site, deploy the station in an area free from human interference, and build a proper seismic vault. These are in the form of applying thermal insulation and ensuring adequate grounding for the broadband seismometer. Most of the seismic noise remains relatively steady over time at most stations, and hence, noise power spectral density can be used effectively to assess station effectiveness. Any outstanding noise spectrum anomalies from the standard noise spectra can also easily reveal instrument failure or errors in the response data [21]. The noise spectra are typically represented as the noise power density acceleration spectrum $P_a(f)$, commonly in units of dB referred to as $10 \log[P_a(f)/(m/s^2)^2/Hz]$. The noise level is calculated by Eq. (1).

$$\text{Noise level} = 10 \log[P_a(f)/(m/s^2)^2/Hz] \quad (1)$$

3.1 Origins of Seismic Noise (Micro-seisms)

The term "micro-seismic" refers to any ground motion (wave) or movement that persists for multiple instances and does not originate from tremors or detonation for an extended period of time [22]. Accurate results are contingent upon the quality of the data captured by the seismometer in addition to the quantity of stations. The noise intensity at each seismometer station is a factor that impacts the integrity of the data. Cultural noise sources, which are derived from human activities, wind, water, and geological sources, are the first two categories of noise sources, and micro-seismic noise is the third type [23]. Seismic noise can be classified into the following categories:

1. Cultural noise: Human activities occurring at or near the Earth's surface constitute the most prevalent origin of seismic noise. The primary source of cultural noise is the transmission of energy from machinery and traffic into the ground. Cultural noise, primarily high-frequency surface waves (1–10 Hz, 1–0.1 s), dissipates over distances and depths of several kilometers. Therefore, tunnels, deep caverns, and boreholes will significantly reduce cultural noise. Cultural noise exhibits notable fluctuations throughout the day and has distinct frequencies that are dependent on the disruption's origin [23].
2. Wind noise: Noise is generated by any object in motion, such as the movement of tree leaves. Topographical features, like slopes or rocks, can disrupt the wind and produce local noise. This noise often appears as high-frequency sounds similar to those generated by human activities. Seismic stations located nearby are particularly affected by this type of noise [23].
3. Ocean-generated noise: commonly encountered in seismic studies, is often called micro-seismic or micro-seismic noise. According to Nishida [24], micro-seismic noise is classified based on its frequency into two categories: Primary micro-seisms, which occur within the frequency range of 0.02 to 0.1 Hz, and secondary micro-seisms, which fall within the frequency range of 0.1 to 0.5 Hz.
4. Additional sources of seismicity include water flowing, surf, volcanic eruptions (which produce an almost coordinated noise associated with fluid motion), or background activity. Thermal instabilities represent another source of noise that exhibits a significant daily variation. Daytime and nighttime temperature variations can induce ground fluctuations, resulting in tilt and long-period noise [25].

4. Power Spectral Density (PSD)

The calculations of PSD estimate the distribution of power with the frequency [17] [26], which is a part of the ObsPy module [27]. It is a common method for measuring seismic background noise and evaluating noise performance. The PSD method is computed by applying the Fast (direct) Fourier Transform or Cooley-Tukey method [28] on the original data, which is a computational technique used for computing the Discrete Fourier Transform (DFT) of a time series. The FFT transforms the time domain signal $y(t)$ to its frequency domain representation, allowing for energy determination at certain frequencies. Eq. (2) is used to calculate the FFT of a continuous series of times $y(t)$ [14] [17].

$$y(f, T) = \int_0^{T_r} y(t) e^{-i2\pi ft} dt \quad (2)$$

where $y(f, T)$ = the frequency-domain representation of the original time-domain signal $y(t)$, f = the frequency that corresponds to various spectral components or sinusoidal waves that constitute the seismic noise signal and T_r = the length of the time series segment.

The frequency estimate is determined using the number of Fourier Transforms with $nfft = (N/2) + 1 = 16385$, where N represents the number of data points in the time series. This ensures a sufficiently high frequency resolution so that the PSD can accurately capture the power distribution across different frequencies [29]. The PSD is repeated for each overlapping time segment, measured in hours. Once the PSD is computed for all segments, the energy is averaged across these segments, where each segment has a duration of T_r , which is described in Eq. (3) [14].

$$P_k = \frac{1}{q} (P_{k,1} + P_{k,2} + \dots + P_{k,q}) \quad (3)$$

To obtain the final PSD, the NLNM and NHNM algorithms are applied, as illustrated in Figure 1, resulting in the final PSD calculated by Eq. (4) [14].

$$P_k = 10 * \log_{10}(P_k) \quad (4)$$

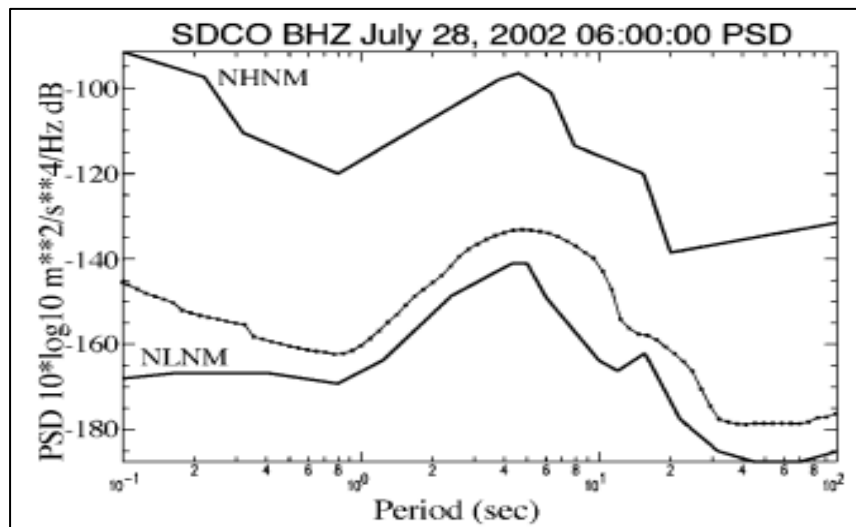


Figure 1: New Representations of Low and High Noise Models (NLNM&NHN M) [17].

5. Probability Density Function (PDF)

A new noise processing software computes statistical PSD density across numerous sub-segments, given as a percentage (%). The United States Geological Survey (USGS) created this algorithm and the initial software as part of the Advanced National Seismic System's data and network quality control (QC) system [17]. The right-hand color scale displays the PDF %. The goal is to understand the genuine variation of noise at a specific station by creating seismic noise PDFs from PSDs and processing them according to the methods discussed in the previous section [17] [30].

Whole octave averages are produced at 1/8 octave intervals to sample the PSDs adequately. This strategy decreases the frequency count by 169, reducing it from 16,385 to 97. The power is averaged between a short-period (high-frequency) threshold, T_s , and a long-period (low-frequency) threshold, $T_l = 2 * T_s$. The centre period, $T_c = \sqrt{T_s * T_l}$, signifies the mean of a geometric period within the octave. These geometric measures are uniformly distributed along a logarithmic scale. The average power level for every interval, which spans the period ranging from T_s to T_l , is saved alongside the central period T_c for later analysis. T_s is then increased by 1/8 octave, resulting in $T_s = T_s * 2^{0.125}$, and the mean power for the following period bin is determined. T_l and T_c are recalculated, and the power is averaged throughout the following period range (T_s to T_l). The procedure remains till a maximum resolved interval is achieved, which is specified by the original data's time series window length $T_r/10$, as shown in Figure 1. This procedure is carried out with each 1-hour PSD computation, resulting in the generation of many thousands of continuous PSD computations for every station element. Power levels are gathered at 1-dB periods to generate a distribution of frequency graphs (histograms) for every period [29].

The distribution of powers per period is then plotted using PDF. The PDF for a specific central period T_c can be calculated using Eq. (5) [29].

$$P(T_c) = \frac{N_{PTc}}{N_{Tc}} \quad (5)$$

where N_{PT_c} = the number of spectral estimates within a 1 dB energy bin P , spanning from -200 to -80 dB, and N_{T_c} = the overall number of spectra estimations during the centre period T_c .

Plotting the probability of a given power occurring at a given time allows for direct comparison with high and low-noise models (Peterson [18]). For every period bin, the lowest, mode, and maximum powers are also computed and shown. This statistical perspective of broadband PDFs provides useful information about seismic noise by showing temporal fluctuations in noise. As background probability levels are typically occupied by system Transients, earthquakes, and general data artifacts, the noise examination program is applied to the complete continual transmission of data without the need to filter them out. Additional information about station quality and the average amount of earth disruption at every location can be gained from artifacts pertaining to station operations and cultural noise events [29]. The output of this noise analysis tool is beneficial for the following purposes: Assessing the present and past effectiveness of existent band instruments, identifying problems with operation inside the system used for recording, and assessing all data accuracy for a specific station. The advantages of a novel method involve the following: the provision of an analytical perspective that illustrates the level of noise in the distribution instead of a simple exact at a minimum, the assessment of the instrument/station's overall condition, and the evaluation of the health of its recording and telemetry systems. Both PSD and PDF methods are calculated by using the obspy tool (library-python) which is used to analyse noise level with the PPSD class [14] [31].

6. Methodology

In this study, we evaluated four stations located in central Iraq through three phases: (i) data collection phase (ii) preprocessing phase, and (iii) analysis phase. In the data collection phase, data were collected from each of the four stations obtained through the installed seismometer device. After collecting the data, it is passed to the pre-processing stage, which includes two basic steps: converting the seismic data files into seismic analysis code (SAC) files and assigning the headers to each SAC file. Following the pre-processing phase, the analysis stage receives the processed data along with the seismometer's response file to correct the instrument response and analyse the seismic noise of the recorded data using the PPSD class to compute PSD and PDF through the Obspy python library. Then, the analysis findings will be compared to the typical Peterson model and plotted for evaluation. Figure 2 illustrates the diagram of a general method for seismic noise data analysis.

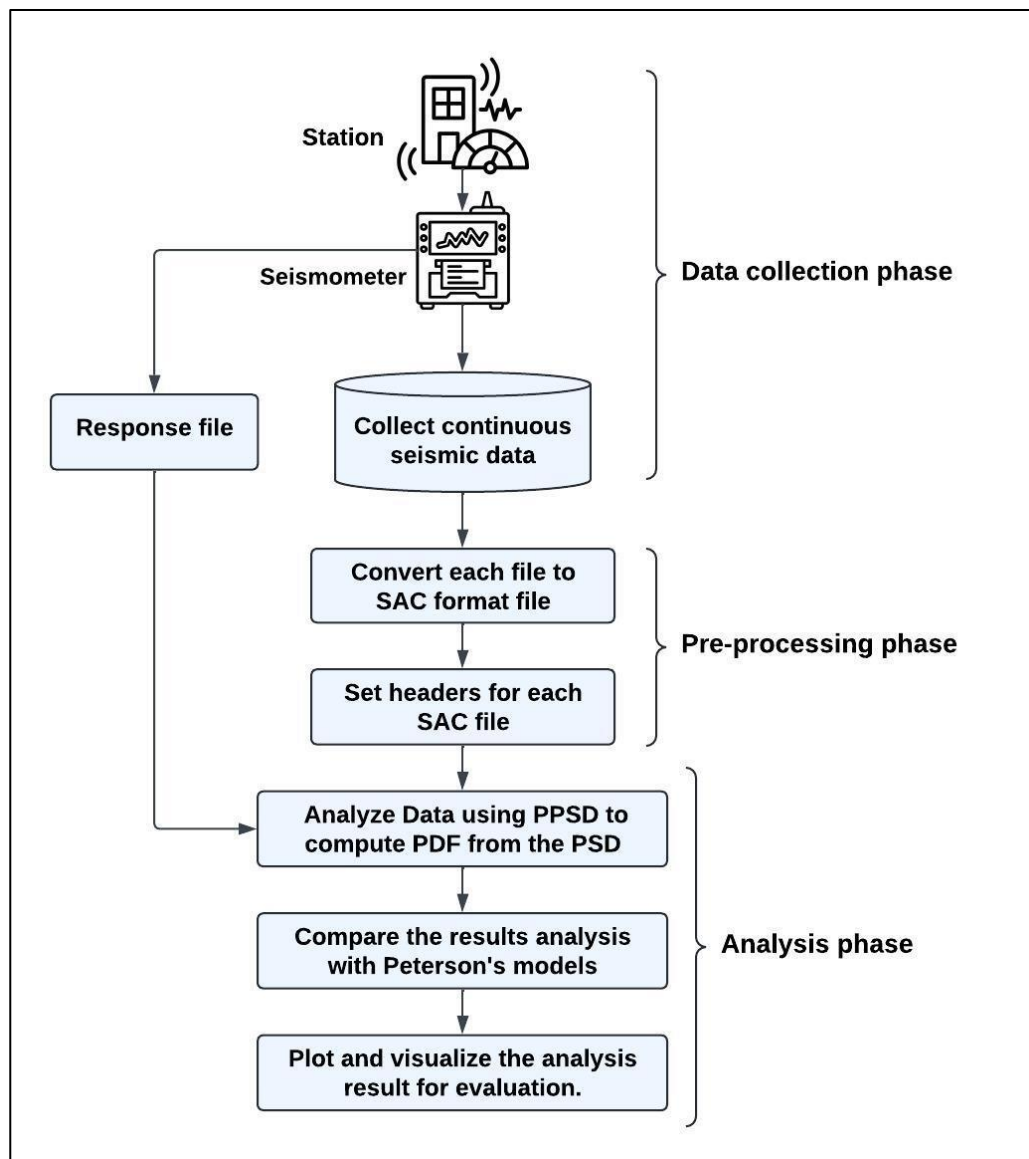


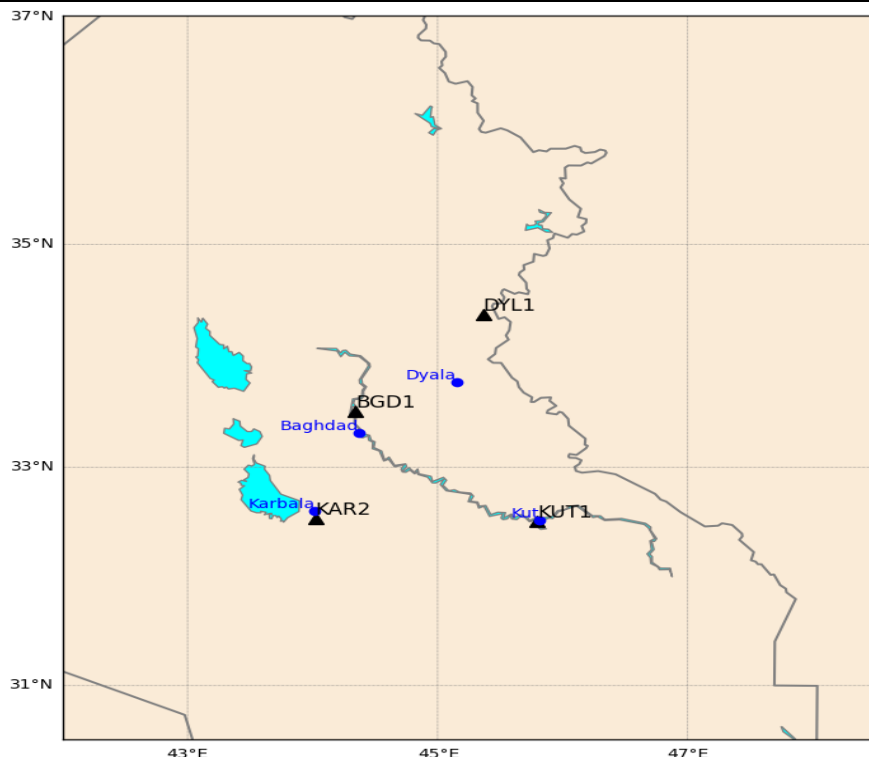
Figure 2: General method for seismic noise data analysis.

6.1 Data collection

Datasets were collected over a one-year period from four stations located in central Iraq, namely Karbala (KAR2), Kut (KUT1), Diyala (DYL1), and Baghdad (BGD1) stations. These seismic stations are part of the Mesopotamian Seismological Network in Iraq (MPSN). Data was obtained through a seismometer installed at each station as shown in Figure 3. A seismometer is a device for recording and capturing seismic wave data in three directions: vertical (Z), north-south (N), and east-west (E). The sensor in the seismometer has a duration ranging from 0.01 to 100 Hz, which allows it to detect a wide spectrum of seismic waves, from low-frequency signals associated with large tectonic events to higher-frequency signals from smaller or local earthquakes. The seismometers installed at KAR2 and KUT1 stations were of the Gürnalp type, which saves seismic data hourly in the Gürnalp compressed format (GCF) file, while the seismometers installed at DYL1 and BGD1 stations were of the Trillium Horizon TH-120 type, which saves seismic data after the file reaches a maximum size of 4000 KB in the minimal standard for the exchange of earthquake data (miniSEED) format. In addition, the response files were also obtained for each instrument. These files contain calibration information and response characteristics of the seismometers, which are crucial for accurately removing the effects of instrument response on the recorded seismic data during analysis. Table 1 illustrates detailed information about four stations located in central Iraq.

Table 1: List of stations located in central Iraq and their corresponding details

Location	Code	Longitude (N)	Latitude (E)	Elevation (m)	Sensor type	Instrument
Karbala 2	KAR2	32.5398	44.0224	45	CMG-40T	Güralp
Kut 1	KUT1	32.5091	45.7974	20	CMG-T3	Güralp
Diyala 1	DYL1	34.3745	45.363	175	Trillium Horizon TH-120	Nanometrics
Baghdad 1	BGD1	33.5092	44.3437	35	Trillium Horizon TH-120	Nanometrics

**Figure 3:** The black triangles show the four seismic stations located in the centre of Iraq.

6.2 Preprocessing

After collecting the dataset from each station, each noise data file was subjected to preprocessing before being analysed, which involved two main steps described in the following:

A. Each seismic data file in GCF format, obtained from the Güralp instrument, was converted into SAC format using the `gcf2sac` tool, a utility developed by Güralp Systems. Güralp Systems specifically designed this tool to convert seismic data from the proprietary GCF (Güralp Compressed Format) to the widely used SAC (Seismic Analysis Code) format for seismic data analysis tasks. Conversely, seismic data files in MiniSEED format from the Trillium Horizon TH-120 instrument were converted directly to SAC format using the `mseed2sac` software brought from the ObsPy library.

B. After converting the data files to SAC format, headers are assigned to each seismic data file using the `gsac` software package [32]. In `gsac` commands, we specified key header values inside each seismic file, namely Longitude (STLO), Latitude (STLA), Elevation (STEL), Station Name (KSTNM), network name (KNETWK) and channel name (KCMPNM). These headers provide critical metadata for accurate interpretation and analysis of the seismic data during the subsequent analysis phase.

6.3 Analysis

During the analysis phase, the prepared seismic data were corrected for instrument response. This was done prior to the generation of seismic noise PDFs from the PSDs via the PPSD class in the Obspy Python library. The method employed implies that the full dataset was collected in 1-hour continuous time slices with a 50% overlap. PSDs are calculated over every segment and channel, and distributions of frequencies are generated by adding the separate PSDs in a certain way: (1) grouping the intervals of 1/8 octave, and (2) grouping the powers into intervals of 1-dB. Then, PDFs are created by normalizing each frequency group to the overall number of PSD. Finally, the analytic results are processed and compared graphically to the Peterson models, which include the upper and lower envelope curves for the NHNM and NLNM. In the case where the noise level of a particular frequency band is above the NHLM, then the seismic signals are regarded as noisy. On the other hand, if the noise levels are below the NLNM then it is referred to as the quiet condition of the signals. For noise levels that lie between the NHLM and NLNM, this means that the station is situated in an area of moderate noise level.

7. Results and Discussion

Seismic noise spans a wide range of frequencies when compared to the NHNM and NLNM models, which are high, low, and intermediate frequencies. During short periods, high-frequency seismic noise is primarily associated with cultural sources such as traffic, construction, and industrial processes; however, over longer periods, it can be influenced by tectonic activity and prolonged wind events that cause vibrations that register as high-frequency signals. Low-frequency seismic noise, on the other hand, is mostly associated with natural phenomena such as ocean waves and atmospheric pressure changes over long periods of time, while in short periods it can be caused by microseisms and local seismic occurrences, reflecting a variety of environmental factors. Intermediate frequency seismic noise in a short period is generated by vibrations from traffic or transportation vehicles and trains, as well as construction activities. Intermediate frequency seismic noise over a long period may be generated due to geological resonances within the Earth's structure or by environmental conditions such as wind and rain that cause prolonged ground oscillations.

The analysis of the signal spectrum (PSD) and PDF for the vertical component (HHZ) at most stations indicates that the level of noise is generally within the acceptable ranges defined by the NHNM and NLNM for periods above 1 s, as shown in Figure 4. However, the PSD plots indicated increasing noise at the shorter periods (0.2-0.9 s) at both Stations BGD1 (Apr- Nov 2023) and KUT1 (Jan 2022- Jan 2023), slightly above the NHNM model, which may be attributed to cultural noise or seasonal noise due to the high temperatures in Iraq, which reach above 50 degrees in the summer season. At the same time, DYL1 station (Feb- Oct 2023) remained within the acceptable noise level, while KAR2 station (Jan 2022- Jan 2023) showed high noise at both high and low period ranges, which is above the NHNM model due to the expansion and the new construction cultural noise throughout the city.

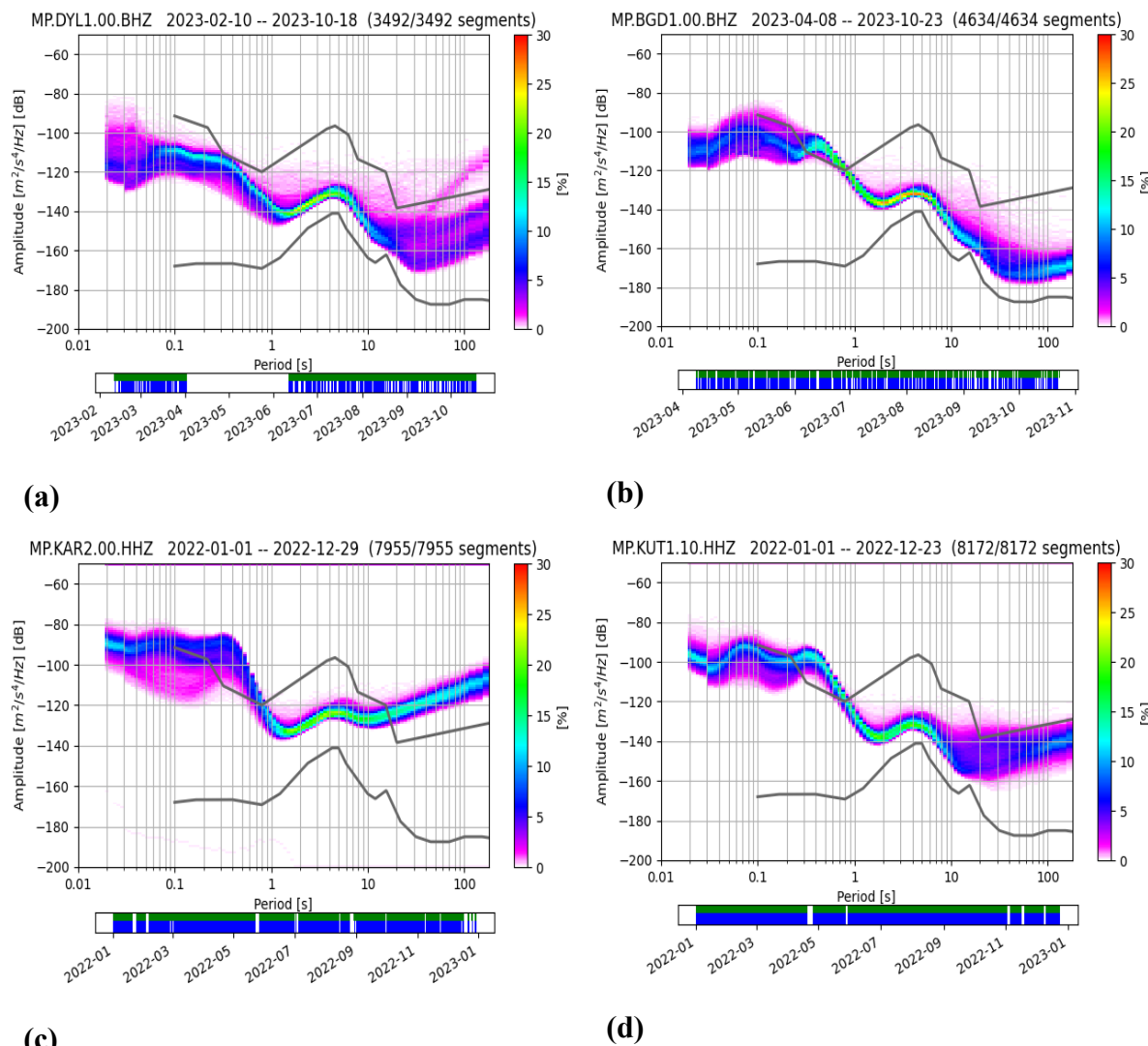


Figure 4: Probabilistic Power Spectral Density (PPSD) results for the vertical component (Z) compared with Peterson's model at (a) DYL1 station, (b) BGD1 station, (c) KAR2 station, and (d) KUT1 station.

The PSD and PDF analyses of the north-south components (N) at the four stations also exhibit similar trends to those seen in the vertical component (Z) analysis, as shown in Figure 5. At Station DYL1 (Feb- Oct 2023), the noise level is within the NHNM and NLNM models at all times, and it is considered acceptable. At periods of 0. 2 to 0. 9 s, the noise levels of both BGD1 (Apr- Nov 2023) and KUT1 (Jan 2022- Jan 2023) stations are slightly elevated and exceed the NHNM. While there is also an increasing trend in the noise levels at station KAR2 (Jan 2022- Jan 2023) for both shorter and longer periods, the noise goes beyond the NHNM, which is also due to urban growth and encroachment.

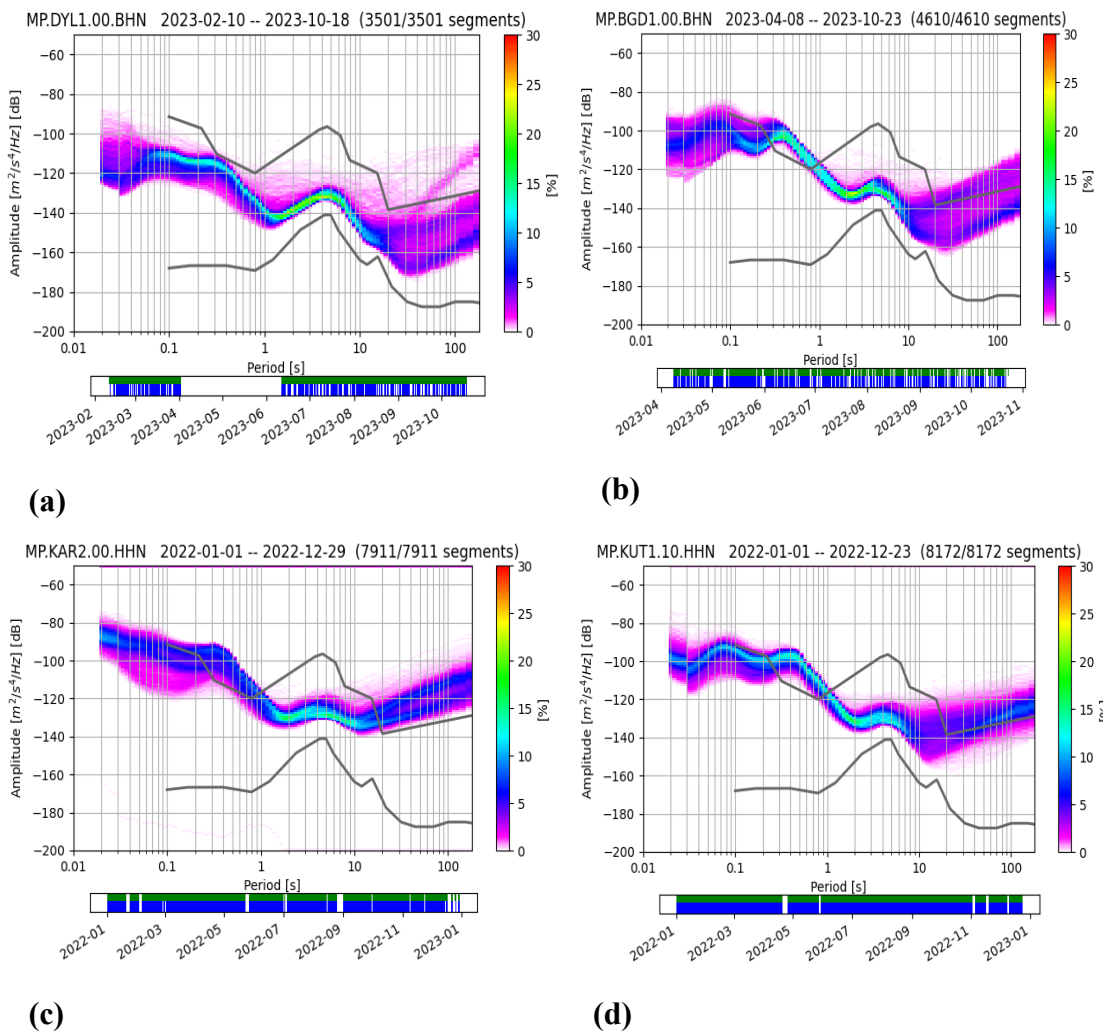


Figure 5: PPSD results for the north-south component (N) compared with Peterson's model at (a) DYL1 station, (b) BGD1 station, (c) KAR2 station, and (d) KUT1 station.

The PSD and PDF analyses of the east-west components (E) at the four stations also exhibit similar trends to those seen in the Z and N component analyses, as shown in Figure 6. At Station DYL1 (Feb- Oct 2023), the noise level is within the NHNM and NLNM models at all times. At periods of 0.3 to 1s, the noise levels of both BGD1 (Apr- Nov 2023) and KUT1 (Jan 2022- Jan 2023) stations are slightly elevated and exceed the NHNM. While there is also an increasing trend in the noise levels at station KAR2 (Jan 2022- Jan 2023), for both shorter and longer periods where the noise goes beyond the NHNM.

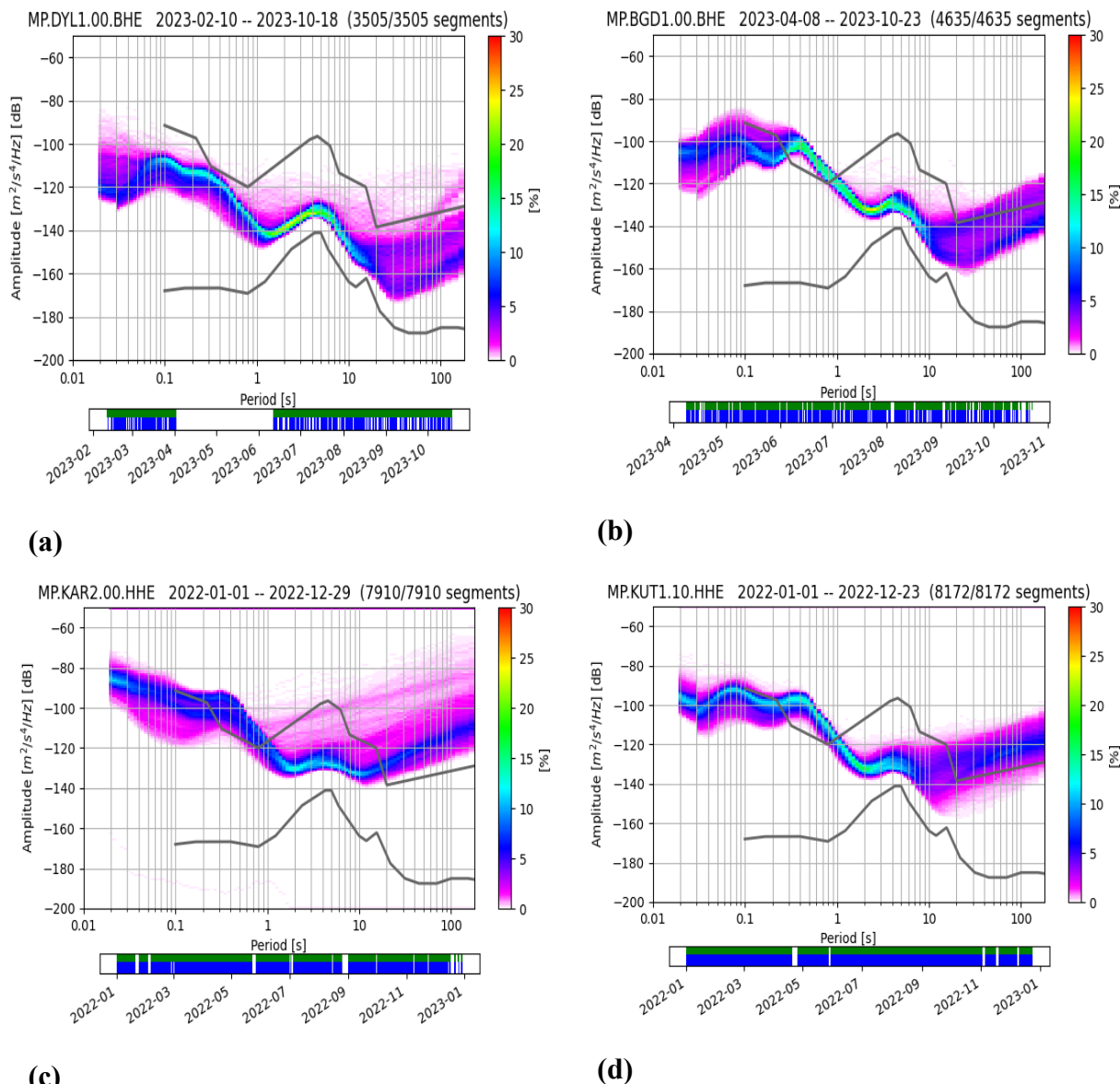


Figure 6: (PPSD) results for the east-west component (E) compared with Peterson's model at (a) DYL1 station, (b) BGD1 station, (c) KAR2 station, and (d) KUT1 station.

In July 2024, a new seismic station in Karbala was installed at the same site. After three months of recording, the noise ratio was recalculated, as shown in Figure 7. The results were similar to those of the previous station; therefore, it is strongly recommended to select a different site for the installation to obtain less noisy data.

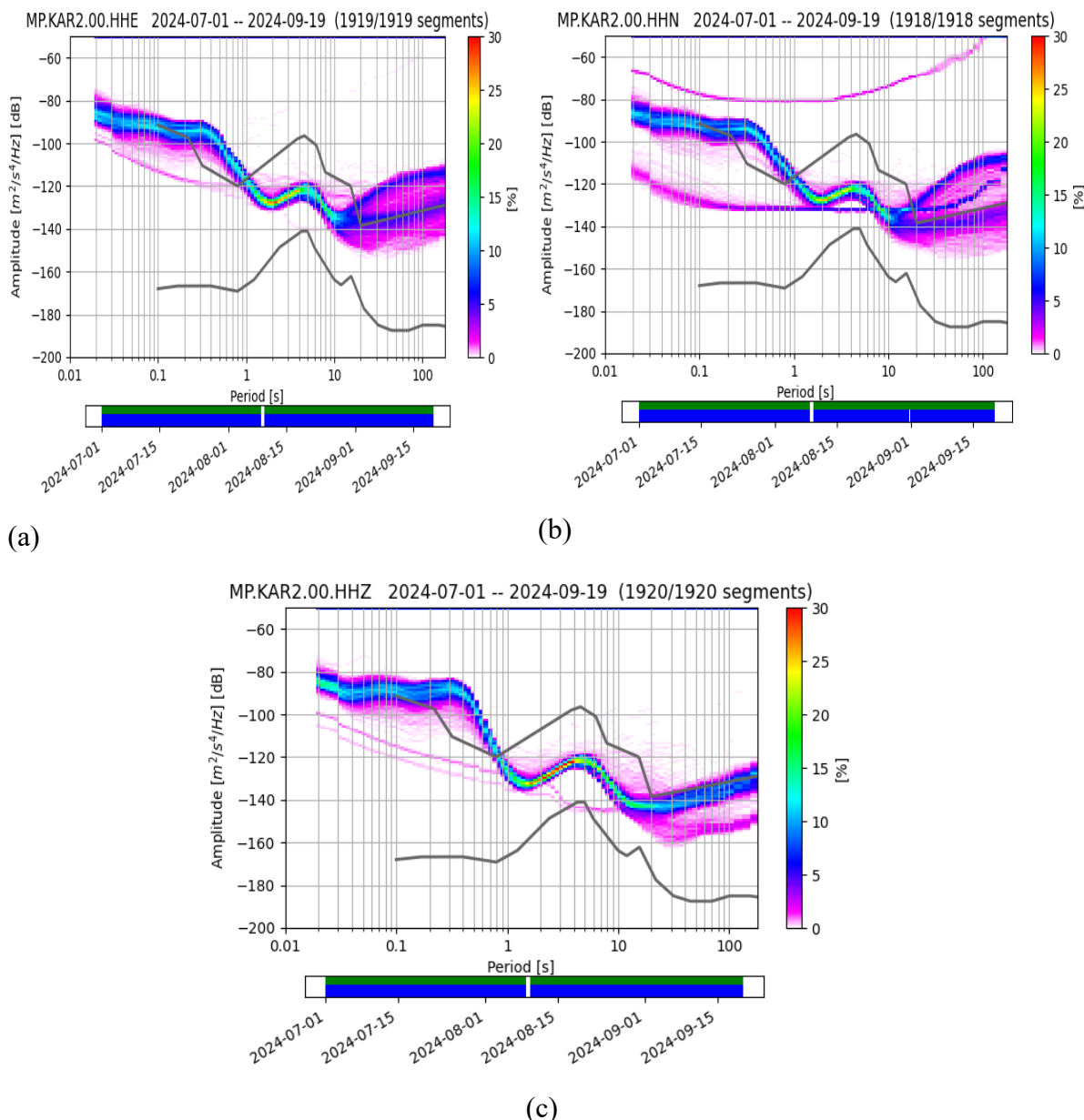


Figure 7: PPSD results for (a) east-west component (E), (b) north-south component (N), and (c) vertical component (Z) compared with Peterson's model at KAR2 station.

8. Conclusion

The noise analysis was successfully evaluated the seismological ambient noise within the selected stations using PSD and PDF methods. The comparison of Power Spectral Density results with Peterson's model revealed except for Karbala station that the installation locations of the seismometers at the other stations were generally successful. Stations BGD and KUT displayed a slight tendency to exceed the NHNM model in the 0.1-1 s frequency range from March to July. This increase is likely attributed to high temperatures typical of the summer season, possibly influenced by cultural factors. This issue can be mitigated using filtering techniques that preserve the integrity of the primary signals. Station DYL maintained noise levels within acceptable throughout all period ranges, indicating an optimal site for earthquake monitoring. In contrast, Station KAR2 showed significantly higher noise levels, especially along the low and high period ranges, likely due to presence of many factors such as urban expansion, heightened local activities and elevated temperatures among others. Thus, relocating the seismometer at Karbala is strongly recommended to minimize noise and enhance

the accuracy of seismic data collection. This study underscores the importance of site selection and monitoring for improving the performance of seismic networks and suggests practical measures for optimizing earthquake detection in central Iraq.

Acknowledgements

I would like to express my invaluable gratitude and appreciation to Dr. Hanan Mahdi and Dr. Haydar Al-Shukri for their guidance, support, and encouragement. I'm also grateful to Muntadher Al-Kaabi for his insightful contributions and collaboration, as well as to the Seismic Monitoring Laboratory members for their encouragement throughout this research. Their assistance has been instrumental in the success of my work.

References

- [1] N. A. Jasim, "Seismicity evaluation of central and southern Iraq," *Iraqi Journal of Science*, vol. 54, no. 4, pp. 911-918, 2013.
- [2] H. E. Abdel Hafiez and M. Toni, "Ambient noise level and site characterization in northern Egypt," *Pure and Applied Geophysics*, vol. 176, pp. 2349-2366, 2019.
- [3] J. Groos and J. Ritter, "Seismic noise: A challenge and opportunity for seismological monitoring in densely populated areas," 2010.
- [4] A. S. Al-Banna, H. H. Majeed, S. S. Al-Karadaghi and S. M. Shalash, "Construction of Regional Seismic Section Along Central Part of Iraq and its Geological Importance," *The Iraqi Geological Journal*, pp. 40-54, 2024.
- [5] K. S. Al Mukhtar and A. A. A. Alsayadi, "Processing and interpretation of 3D seismic data of an oil field in central of Iraq using AVO techniques," *Iraqi Journal of Science*, pp. 1728-1738, 2015.
- [6] H. H. Hasan, W. M. Arif and E. A. Sulaiman, "Seismic analysis of RC building with plan irregularity in Baghdad/Iraq to obtain the optimal behavior," *Open Engineering*, vol. 14, no. 1, p. 20240003, 2024.
- [7] Z. Ghemari, "Comprehensive Signal Analysis: Unraveling Mean Frequency, Power, and Bandwidth," *J Mod Ind Manuf*, vol. 3, no. 4, 2024.
- [8] B. Isaías, C. J. Andrés and J. Tago, "Modelling Evolutionary Power Spectral Density Functions of Strong Earthquakes Via Copulas," *arXiv preprint arXiv:2403.13959*, 2024.
- [9] B. Grecu, C. Neagoe, D. Tataru, F. Borleanu and B. Zaharia, "Analysis of seismic noise in the Romanian-Bulgarian cross-border region," *Journal of Seismology*, vol. 22, pp. 1275-1292, 2018.
- [10] T. Rahayu, R. Sipayung, A. R. Ainun, M. Sinambela and K. Tarigan, "An Application of Power Spectral Density and Probability Density Function for Seismic Mini Region Stations Performance: Padang Lawas Earthquake," 2020.
- [11] M. Sinambela, M. Situmorang, K. Tarigan, S. Humaidi, H. Rumapea, N. F. Saragih, S. Sitepu, I. K. Jaya and T. Rahayu, "Detection of Background Seismic Noise on Selected Digital Broadband Network Stations: Tarutung Earthquake," 2020.
- [12] S. Saha and D. Srinagesh, "Seismic noise characteristics of Maitri broadband seismic station in Antarctica: using power spectral density estimation," 2021.
- [13] A. R. Hakim, A. H. Saputro, S. Rohadi, M. T. Gunawan and R. Kardoso, "Seismic Noise Analysis in InaTEWS Earthquake Station Network (Case Study: Flores Earthquake 7.4, 14 December 2021)," 2022.
- [14] D. Agusdiansyah, Y. Yuliastuti, T. A. Ryanto, A. M. Haifani and N. Nurlaila, "Comparative ambient noise analysis using probability spectral density of Bangka seismic network," *Jurnal Sains dan Teknologi Nuklir Indonesia (Indonesian Journal of Nuclear Science and Technology)*, vol. 23, no. 2, pp. 43-50, 2023.
- [15] K. Jha, "Analysis of seismic noise of broadband seismological stations installed along the Western Ghats," *Journal of Seismology*, vol. 27, no. 2, pp. 325-342, 2023.

- [16] R. C. Aster, D. E. McNamara and P. D. Bromirski, "Multidecadal climate-induced variability in microseisms," *Seismological Research Letters*, vol. 79, no. 2, pp. 194-202, 2008.
- [17] D. E. McNamara and R. P. Buland, "Ambient noise levels in the continental United States," *Bulletin of the seismological society of America*, vol. 94, no. 4, pp. 1517-1527, 2004.
- [18] J. Peterson, "Observations and modeling of seismic background noise," *US Geological Survey*, pp. No. 93-322, 1993.
- [19] A. El-Aziz K. Abd El-Aal And M. S. Soliman, "New Seismic Noise Models Obtained Using Very Broadband Stations," *Pure Appl Geophys*, vol. 170, pp. 1849-1857, 2013.
- [20] B. G. C. N. I. A. M. A. V. E. T. A. Tolea, "Seismic Noise Analysis In The Microseismic And High-Frequency Domain At The Burar Seismic Stations," *Rom Rep Phys*, vol. 75, p. 705, 2023.
- [21] R. S. Yuliatmoko, M. T. Gunawan, M. Adi, A. Wijaya, R. A. P. Kambali, T. Kurniawan, D. K. Karnawati and S. Rohadi, "Seismic Station Quality Monitoring and Evaluation System in Indonesia," 2023.
- [22] B. Gutenberg, "Microseisms," vol. 5, Elsevier, 1958, pp. 53-92.
- [23] J. Havskov and G. Alguacil, "Seismic recorders," Springer, 2004, pp. 113-149.
- [24] K. Nishida, "Ambient seismic wave field," *Proceedings of the Japan Academy, Series B*, vol. 93, no. 7, pp. 423-448, 2017.
- [25] R. Contreras-Arratia and J. W. Neuberg, "Complex seismic sources in volcanic environments: Radiation modelling and moment tensor inversions," *Journal of Volcanology and Geothermal Research*, vol. 381, pp. 262-272, 2019.
- [26] S. Custódio, N. A. Dias, B. Caldeira, F. Carrilho, S. Carvalho, C. Corela, J. Díaz, J. Narciso, G. Madureira and L. Matias, "Ambient noise recorded by a dense broadband seismic deployment in western Iberia," *Bulletin of the Seismological Society of America*, vol. 104, no. 6, pp. 2985-3007, 2014.
- [27] L. Krischer, T. Megies, R. Barsch, M. Beyreuther, T. Lecocq, C. Caudron and J. Wassermann, "ObsPy: A bridge for seismology into the scientific Python ecosystem," *Computational Science & Discovery*, vol. 8, no. 1, p. 014003, 2015.
- [28] J. W. Cooley and J. W. Tukey, "An algorithm for the machine calculation of complex Fourier series," *Mathematics of computation*, vol. 19, no. 90, pp. 297-301, 1965.
- [29] D. E. McNamara and R. I. Boaz, Seismic noise analysis system using power spectral density probability density functions: A stand-alone software package, US Geological Survey Reston, Virginia, 2006.
- [30] J. Díaz, A. Villaseñor, J. Morales, A. Pazos, D. Córdoba, J. Pulgar, J. L. García-Lobón, M. Harnafi, R. Carbonell and J. Gallart, "Background noise characteristics at the IberArray broadband seismic network," *Bulletin of the Seismological Society of America*, vol. 100, no. 2, pp. 618-628, 2010.
- [31] M. R. Koymans, J. Domingo Ballesta, E. Ruigrok, R. Sleeman, L. Trani and L. G. Evers, "Performance assessment of geophysical instrumentation through the automated analysis of power spectral density estimates," *Earth and Space Science*, vol. 8, no. 9, p. e2021EA001675, 2021.
- [32] R. B. Herrmann, "Computer programs in seismology: An evolving tool for instruction and research," *Seismological Research Letters*, vol. 84, no. 6, pp. 1081-1088, 2013.